Corneal Epithelial Cells Exhibit Myeloid Characteristics and Present Antigen via MHC Class II

Derek J. Royer,[1] Michael H. Elliott,[1,2] Yun Z. Le,[1,3–5] and Daniel J. J. Carr[1,6]

[1]Department of Ophthalmology, University of Oklahoma Health Sciences Center, Oklahoma City, Oklahoma, United States
[2]Department of Physiology, University of Oklahoma Health Sciences Center, Oklahoma City, Oklahoma, United States
[3]Department of Cell Biology, University of Oklahoma Health Sciences Center, Oklahoma City, Oklahoma, United States
[4]Department of Internal Medicine, University of Oklahoma Health Sciences Center, Oklahoma City, Oklahoma, United States
[5]Harold Hamm Diabetes Center, University of Oklahoma Health Sciences Center, Oklahoma City, Oklahoma, United States
[6]Department of Microbiology and Immunology, University of Oklahoma Health Sciences Center, Oklahoma City, Oklahoma, United States

Correspondence: Derek J. Royer, Department of Ophthalmology, Dean McGee Eye Institute, Acers Pavilion Room 419, 608 Stanton L. Young Boulevard, Oklahoma City, OK 73104, USA; Derek-Royer@ouhsc.edu; Derek.Royer@Duke.edu, after April 16, 2018.

Submitted: November 2, 2017
Accepted: February 10, 2018

Citation: Royer DJ, Elliott MH, Le YZ, Carr DJJ. Corneal epithelial cells exhibit myeloid characteristics and present antigen via MHC Class II. *Invest Ophthalmol Vis Sci*. 2018;59:1512–1522. https://doi.org/10.1167/iovs.17-23279

Purpose. To explore the impact of ocular surface insults on the immunomodulatory capacity and phenotype of corneal epithelial cells (CECs) with a focus on epithelial–mesenchymal transition (EMT).

Methods. Corneas were harvested from mice 6 days following scratch injury, ragweed pollen–induced allergy, or herpes simplex virus type 1 (HSV-1) infection and compared to healthy tissue controls. Corneas were enzymatically digested and CECs phenotypically characterized using flow cytometry. CECs were defined as epithelial cell adhesion molecule (EpCAM)-positive CD45-negative cells. CECs were assessed by PCR to evaluate EMT-associated transcripts. Recombinant HSV-1 and transgenic mice were utilized to investigate the role of vascular endothelial growth factor A (VEGFA) on the phenotype observed. The immunomodulatory potential of CECs was assessed in coculture assays with ovalbumin-specific CD4 T cells.

Results. Ectopic expression of classic "myeloid" antigens Ly6G, CCR2, and CX3CR1 was identified in CEC subsets from all groups with evidence supporting an underlying partial EMT event resulting from loss of cell–cell contacts. Corneal HSV-1 infection induced Ly6C expression and major histocompatibility complex (MHC)-II upregulation in CECs through a VEGFA-linked mechanism. These $Ly6C^{+}$ $MHC\text{-}II^{+}$ CECs were found to function as amateur antigen-presenting cells and induced CD4 T cell proliferation in vitro.

Conclusions. This study characterizes a novel immunomodulatory CEC phenotype with possible implications for immune privilege, chronic inflammation, and tissue fibrosis. Moreover, the identification of CECs masquerading with multiple "myeloid" antigens warrants careful evaluation of flow cytometry data involving corneal digests.

Keywords: immunoregulation, herpes simplex virus type 1, corneal epithelium, epithelial-mesenchymal transition

Mucosal epithelial cells form protective barriers and help regulate local inflammatory responses.[1–3] Conversely, epithelial barrier dysfunction exacerbates inflammatory diseases in a variety of mucosal sites including the airways, gut, and ocular surface.[4–6] Niche-specific microenvironmental cues regulate epithelial cell differentiation and function in health and disease.[7–9] At the ocular surface, corneal epithelial cells (CECs) modulate many inflammatory diseases across the life span and are essential for maintaining corneal immune privilege, avascularity, and visual acuity.[10–13] Tightly regulated transcriptional programs in CECs facilitate homeostatic barrier integrity and proper histoanatomic organization of the cornea.[14,15] While healthy CECs undergo continual turnover and renewal, pathologic changes in the corneal epithelium or its progenitor stem cell niche contribute to vision loss and significantly affect quality of life.[16,17] However, the immunologic impacts of CECs are incompletely understood in ocular surface diseases.

Cellular plasticity is essential for normal tissue development, maintenance, and repair. However, insults such as mechanical injury, inflammation, and infection can induce aberrant cellular reprogramming and transdifferentiation. Epithelial–mesenchymal transition (EMT) is one such phenomenon involved in development, wound healing/fibrosis, and malignancy/metastatic transformation.[18] Several viruses have also been reported to elicit EMT including human papilloma virus,[19] Epstein-Barr virus,[20] hepatitis B virus,[21] and hepatitis C virus.[22] During EMT, epithelial cells undergo dynamic transcriptional changes affecting adhesion, polarity, and survival.[23] In addition, the possibility of "epithelial to myeloid" transition has been considered due to the phenotypic overlap between many mesenchymal- and myeloid-associated antigens.[24–26] This proposition is further supported by similar chemokine-dependent mechanisms of leukocyte dissemination through lymphatic vessels and lymphatic metastasis of malignant cells arising from EMT.[27]

In this article, we investigate the hypothesis that herpes simplex virus type 1 (HSV-1) mediates EMT in CECs. Our work stems from a serendipitous observation that cells sort-purified from HSV-1-infected corneal digests contained a heterogeneous population of Ly6G-positive (antibody clone 1A8) and Ly6C-postive cells (antibody clone HK1.4) including many with epithelioid morphology. However, Ly6G and Ly6C are widely regarded as murine "neutrophil" and "monocyte" markers, respectively. Both Ly6G and Ly6C are GPI-anchored cell surface proteins that lack human orthologs.[28] While the function of these proteins is unclear, Ly6G and Ly6C expression is associated with leukocyte recruitment and homing.[29,30] We have recently shown that CD326/epithelial cell adhesion molecule (EpCAM) is an excellent cell-surface marker for identifying CECs by flow cytometry—circumventing the need for intracellular cytokeratin staining.[31] In the same study, we found that HSV-1 infection leads to an acute increase in the total number of CECs,[31] but the phenotype and physiology of these CECs originating under inflammatory conditions have not been characterized. Here, we investigate ectopic "myeloid" antigen expression on CECs as a possible outcome of EMT following ocular surface injury, allergy, and HSV-1 infection and explore the downstream immunologic consequences.

Materials and Methods

Animals

Eight- to 16-week-old male and female mice were used for experiments; sexes are recorded in each figure legend. Animals were housed in the Dean McGee Eye Institute's specific-pathogen-free vivarium for at least 1 week prior to experimentation. Wild-type (WT) C57BL/6 and OT-II TCR transgenic mice were obtained from the Jackson Laboratory (Bar Harbor, ME, USA). Transgenic C57BL/6-background alpha smooth muscle actin GFP-reporter mice (α-SMA-GFP)[32] were bred in-house. Transgenic C57BL/6-background mice expressing a floxed vascular endothelial growth factor A allele ($Vegfa^{flox}$)[33,34] were bred within our institution's Rodent Barrier Facility and were originally provided by Genentech (South San Francisco, CA, USA). Mice were anesthetized by intraperitoneal (IP) injection with xylazine (6.6 mg/kg) and ketamine (100 mg/kg) for all procedures and euthanized by exsanguination via intracardiac perfusion with 10 mL PBS prior to tissue collection. The Institutional Animal Care and Use Committee at the University of Oklahoma Health Sciences Center approved all procedures. Experiments were conducted in accordance with the ARVO Statement for the Use of Animals in Ophthalmic and Vision Research.

Corneal Disease Models

Allergic keratoconjunctivitis was induced with short ragweed (*Ambrosia artemisiifolia*) pollen (SRP) from Greer Labs (Lenoir, NC, USA) as previously described,[35] with modifications. Briefly, mice were immunized by footpad injection with 50 μg SRP in 25 μL Imject alum (Thermo Fisher Scientific, Waltham, MA, USA). Ten days later, mice were subjected to daily topical treatments of 0.25 mg SRP in 5 μL PBS in both eyes for 6 days. For the corneal scratch injury model (mock infection control), the corneal epithelium of both eyes was partially debrided with a 25-gauge needle and blotted to remove the tear film. Mice were infected with HSV-1 by applying an inoculum of virus in 3 μL PBS to each eye following partial epithelial debridement (described above). Unless otherwise indicated, HSV-1 infection was mediated using 1×10^4 plaque-forming units (PFU) HSV-1 McKrae per eye and corneas were harvested at day 6 post infection (p.i.). Studies with $Vegfa^{flox}$ mice were conducted using 1×10^3 PFU HSV-1 SC16 or a recombinant derivative expressing Cre recombinase under the ICP0 promoter as described elsewhere.[33,34,36]

Cell Isolation and Flow Cytometry

Corneas were cut from enucleated eyes to exclude the vascularized limbus and digested into single-cell suspensions for analysis as previously described.[31] Briefly, corneas were enzymatically digested in Liberase TL enzyme mix (Roche Diagnostics, Indianapolis, IN, USA) and filtered through 40-μm mesh. Corneal digests were incubated with eBioscience anti-CD16/CD32 Fc block (Thermo Fisher Scientific) and EpCAM- or CD45-expressing cells labeled with immunomagnetic beads and isolated by positive selection using MS or LS cell separation columns (Miltenyi Biotec, Bergish Gladbach, Germany) according to the manufacturer's directions. Isolated cells were labeled with eBioscience antibodies (Thermo Fisher Scientific) for phenotypic profiling and washed in PBS containing 1% bovine serum albumin. For cell cycle analysis, mice were injected with 1.5 mg bromodeoxyuridine (BrdU) IP at the time of infection. Cornea-derived $EpCAM^+$ cells were then isolated and labeled with anti-BrdU and 7-aminoactinomycin D (7-AAD) using a commercial flow cytometry kit according to the manufacturer's directions (BD Biosciences, San Jose, CA, USA). Intracellular labeling for FoxP3 and IFNγ was performed using the eBioscience transcription factor staining kit (Thermo Fisher Scientific) according to the manufacturer's instructions. A MACSQuant 10 flow cytometer and MACSQuantify software were utilized to analyze all samples (Miltenyi Biotec). Gating boundaries were established using isotype labeling, fluorescence minus one, or biological negative controls. For coculture assays, CD4 T cells were sorted from the spleens of OT-II TCR transgenic mice using a Biorad S3e cell sorter (Hercules, CA, USA).

Immunohistochemistry and Microscopy

Corneas were prepared as previously described for imaging.[31] Briefly, corneas were fixed in 4% paraformaldehyde, permeabilized in 1% Triton X-100 (Sigma-Aldrich Corp., St. Louis, MO, USA), blocked with anti-CD16/32, and labeled using a biotinylated anti-EpCAM antibody (eBioscience, Thermo Fisher Science) with a streptavidin–rhodamine conjugate (Jackson ImmunoResearch, West Grove, PA, USA). Filamentous actin and nuclei were stained using Alexa Fluor 488–conjugated phalloidin (Life Technologies, Carlsbad, CA, USA) and 4′,6-diamidino-2-phenylindole (DAPI), respectively. An Olympus FV1200 confocal microscope was used for immunofluorescence image acquisition using sequential channel scanning mode (Center Valley, PA, USA). Phase contrast imaging of isolated $EpCAM^+$ cells was performed using an Olympus IX71 microscope at ×32 magnification following cytospin preparation with a Wescor Cytopro 7620 cytocentrifuge (Logan, UT, USA).

Semiquantitative PCR

For analysis of EMT-associated transcripts, total RNA was isolated from $EpCAM^+$ cells using the Trizol reagent (Thermo Fisher Scientific) method and converted to cDNA with iScript (Biorad). Gene amplification was conducted by real-time PCR using a Biorad CFX-Connect thermocycler and PrimePCR technology with commercially validated proprietary primer sequences (Biorad) according to the manufacturer's directions. Relative expression was normalized to uninfected controls

Investigative Ophthalmology & Visual Science

using the $2^{-\Delta\Delta Ct}$ method with *GAPDH* (glyceraldehyde 3-phosphate dehydrogenase) used as an internal reference gene.

Phagocytosis Assay

Freshly isolated neutrophils were cocultured with pHrodo green–labeled *Escherichia coli* bioparticles (Invitrogen, Carlsbad, CA, USA) at 37°C for 1 hour in 24-well plates containing 500 µL culture media to establish detection parameters for endocytosis by flow cytometry. Culture media consisted of RPMI 1640–supplemented 10% heat-inactivated fetal bovine serum, 10 µg/mL gentamicin, 1× antibiotic/antimycotic (Invitrogen). In order to obtain neutrophils, mice were injected IP with 0.09 g casein in PBS (Sigma-Aldrich Corp.) to elicit a neutrophilic inflammatory response overnight. Neutrophils were collected the following day by peritoneal lavage with 5 mL warm PBS 1 hour following a second IP casein injection as described.[37,38] To assess endocytosis of corneal cells, whole corneal digests were incubated with pHrodo green–labeled *E. coli* bioparticles at 37°C for 1 hour in 24-well plates containing 500 µL culture media. Cells were then immunolabeled and analyzed by flow cytometry.

Lymphocyte Proliferation Assay

Cocultures of sequentially isolated $CD45^+$ and $EpCAM^+$ cells from healthy or HSV-1–infected corneas were established in 500 µL culture media containing 5 µg/mL acyclovir (Sigma-Aldrich Corp.) in 24-well plates. Each culture contained one-cornea equivalent of $EpCAM^+$ cells, two-cornea equivalents of $CD45^+$ cells, or no corneal cells (negative control) in the presence of 10 µg $OVA_{323\text{-}339}$ peptide (EZ-Biolab, Carmel, IN, USA) and 1×10^5 FACS-purified transgenic OT-II CD4 T cells prelabeled in 1 µM carboxyfluorescein succinimidyl ester (CFSE; Thermo Fisher Scientific). Proliferation of the OT-II CD4 T cells was assessed by flow cytometry after incubating for 40 hours at 37°C with 5% CO_2. Plates were incubated for 5 additional hours following addition of 0.5 µL/culture Golgi-stop (BD Biosciences) to assess IFNγ production and FoxP3 expression.

Statistical Analysis

Data shown on bar graphs reflect mean ± SEM. Prism 5 software (GraphPad, San Diego, CA, USA) was used for statistical analysis, and the tests utilized are described in each figure legend. Significance thresholds for comparisons are as follows: $^*P < 0.05$, $^{**}P < 0.01$, $^{***}P < 0.001$. Distinctions in sex are noted where statistically significant differences were identified between male and female mice.

Supplementary Materials

Supplementary data provide a time-course study highlighting the kinetics of Ly6C and Ly6G expression in CECs from HSV-1–infected corneas (Supplementary Fig. S1) and the cell cycle distribution of corneal $EpCAM^+$ $CD45^+$ Langerhans cells (Supplementary Fig. S2).

Results

Corneal Epithelial Cells Express Select "Myeloid" Antigens

Ubiquitous intercellular EpCAM expression was observed in the corneal epithelium of C57BL/6 mice as shown by confocal microscopy (Fig. 1A). Corneas were harvested and digested and $EpCAM^+$ cells isolated using immunomagnetic beads. Flow cytometry was utilized to phenotypically characterize the putative expression of Ly6C and Ly6G in the $EpCAM^+$ CECs from healthy corneas and 6 days following superficial epithelial scratch injury (mock infection), ragweed pollen–induced allergic keratoconjunctivits, or HSV-1 infection (Fig. 1B). Doublets and $EpCAM^+$ $CD45^+$ leukocytes (Langerhans cells) were excluded from analysis (Fig. 1B). Ectopic expression of Ly6G was observed in a subset of CECs from all experimental groups, although a population of CECs from mice ocularly infected with HSV-1 exhibited stark upregulation of Ly6C relative to healthy or epithelial scratch controls (Fig. 1B). Isotype controls for anti-Ly6C (HK1.4) and anti-Ly6G (1A8) were included to rule out nonspecific antibody binding in CECs from HSV-1–infected mice (Fig. 1C). Furthermore, ectopic Ly6C expression was identified in CECs from HSV-1–infected corneas as early as day 3 p.i. (Supplementary Fig. S1).

Isolated $EpCAM^+$ cells exhibited a mixed epithelioid morphology (Fig. 1D); however, flow cytometry–based antibody profiling for other common myeloid antigens was performed to further characterize the $Ly6G^+$ CECs from healthy and HSV-1–infected corneas (Fig. 1E). Notably, the chemokine receptor CCR2 was upregulated in $Ly6G^+$ CECs from healthy and HSV-1–infected corneas, and the fractalkine receptor CX3CR1 was expressed in $Ly6G^+$ and $Ly6G^-$ CECs from both groups (Fig. 1E). Other common leukocyte/macrophage antigens were not detected on the CECs, including CD11b, CD11c, CSF1R, CXCR3, or LYVE1 (data not shown). Given the ectopic expression of select myeloid antigens in CECs, we investigated the hypothesis that HSV-1 drives EMT-associated cellular reprogramming and immunomodulation.

The Epithelial $Ly6C^+$ Phenotype Induced by HSV-1 Diverges From Classical EMT

Cellular reprogramming associated with EMT involves cell cycle changes concomitant with a progressive loss of epithelial markers and induction of a mesenchymal phenotype.[23] Flow cytometry–based cell cycle analysis of $EpCAM^+$ $CD45^-$ cell populations revealed distinct profiles based on BrdU and 7-AAD labeling (Fig. 2A). Although nearly half of the $Ly6G^-$ $Ly6C^-$ CECs from healthy and HSV-1–infected corneas were dead/apoptotic, the majority of viable $Ly6G^-$ $Ly6C^-$ cells from both groups were in the G0/G1 state (Fig. 2B, left). Fewer dead/apoptotic cells were observed in the $Ly6G^+$ $Ly6C^-$ CEC population from both groups with a greater proportion of these cells exhibiting a shift to the G2/M profile (Fig. 2B, middle). The staining pattern among the $Ly6G^+$ $Ly6C^+$ CECs following HSV-1 infection reflected the $Ly6G^+$ $Ly6C^-$ subset with a dominant G2/M phenotype (Fig. 2B, right). Few cell cycle differences were observed between CEC subpopulations from healthy and HSV-1–infected corneas, although enhancement of the G2/M population was noted among all $Ly6G^+$ CECs. Incidentally, 60% of the corneal $C45^+$ $EpCAM^+$ Langerhans cells were in S phase (Supplementary Fig. S2)—consistent with their self-renewal capacity in the epidermis.[39]

Other characteristics of EMT were subsequently explored in $Ly6G^+$ CECs exhibiting a G2/M phenotype, as G2 phase cell cycle arrest is associated with partial EMT and fibrosis in some contexts.[40] Epithelial (E)-cadherin expression was diminished in the $Ly6G^+$ CEC population from healthy and HSV-1–infected corneas relative to the corresponding $Ly6G^-$ populations (Fig. 2C). However, the mesenchymal marker α-smooth muscle actin (α-SMA) was detected only in a small population of $Ly6G^-$ CECs following HSV-1 infection as determined using transgenic α-SMA-GFP reporter mice (Fig. 2D). Semiquantitative RT-PCR was performed to evaluate other EMT-associated transcripts in $EpCAM^+$ cells isolated from healthy, HSV-1–infected, or mock-infected (scratch control) corneas (Fig. 2E). Several transcripts

Investigative Ophthalmology & Visual Science

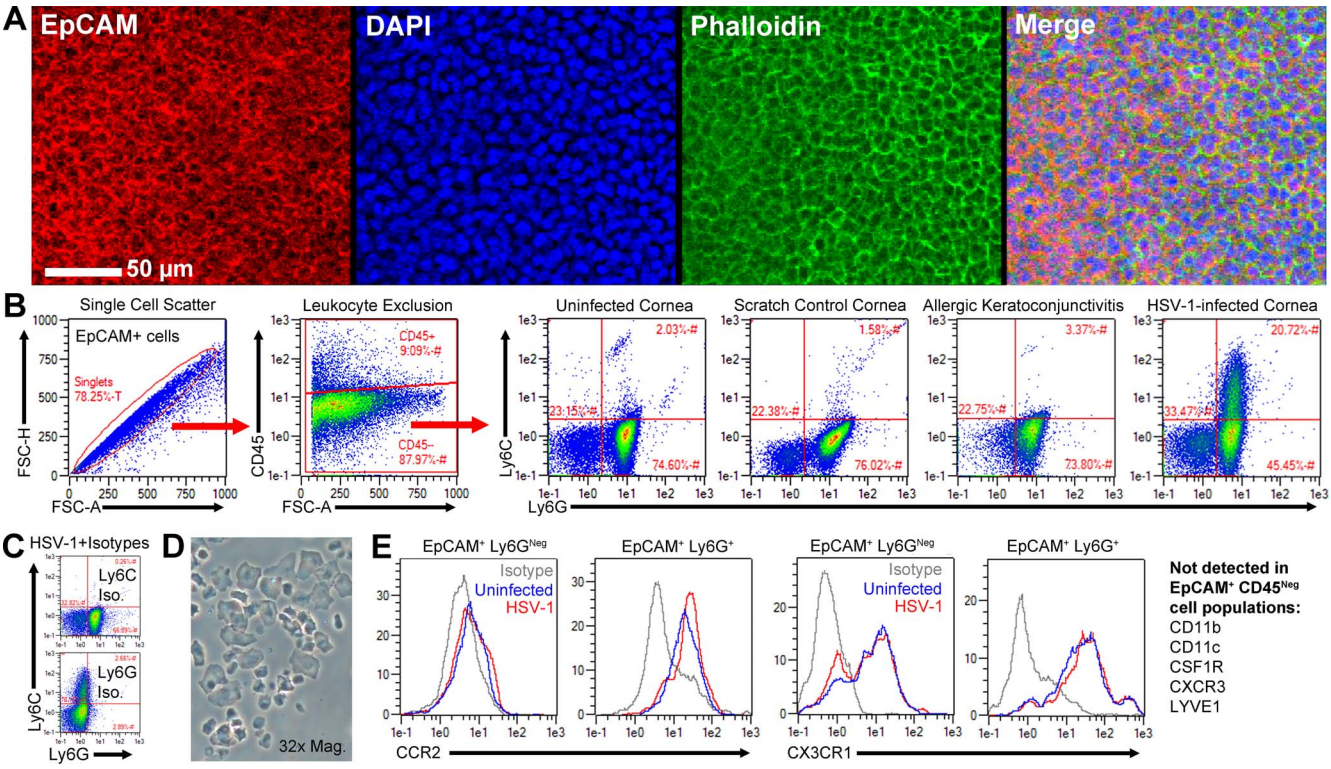

Figure 1. Corneal epithelial cells express select "myeloid" antigens. (**A**) Representative confocal micrograph depicting EpCAM expression in the epithelium of a corneal whole mount with DAPI and phalloidin staining for nuclei and cell boundaries, respectively. *Scale bar*: 50 µm. (**B**) Flow cytometry gating strategy utilized to characterize isolated $CD45^-$ $EpCAM^+$ corneal epithelial cells (CECs) including exclusion of doublets and $CD45^+$ cells followed by analysis of Ly6C (HK1.4) and Ly6G (1A8) expression. Representative dot plots are shown for CECs from healthy corneas, mock infection (scratch control), short ragweed pollen–induced allergic keratoconjunctivitis, and HSV-1 infection (1×10^4 PFU HSV-1 McKrae per eye) reflecting at least four mice per group from at least two independent experiments with male and female animals. Cornea pairs were collected and processed together 6 days post injury/infection or after 6 days of repeated topical allergen challenge. (**C**) Isotype controls for Ly6C and Ly6G labeling of CECs isolated from HSV-1–infected corneas. (**D**) Phase contrast micrograph of isolated $EpCAM^+$ cells from HSV-1–infected corneas (×32 magnification). (**E**) Flow cytometry histograms depicting CCR2 and CX3CR1 expression in $Ly6G^+$ and $Ly6G^-$ CECs from healthy (*blue*) and HSV-1–infected (*red*) corneas as in (**B**). Isotype labeling (*gray*) was conducted using CECs from HSV-infected corneas. Data are representative of two independent experiments with three male mice per group.

fell below the detection threshold, although expression of the EMT-associated transcription factors Snai2 and Twist was identical among $EpCAM^+$ cells from healthy, scratch control, and HSV-infected corneas (Fig. 2E). However, expression profiles corroborated Ly6C and IFNβ upregulation in $EpCAM^+$ cells from HSV-1–infected corneas (Fig. 2E). These findings collectively indicate that acute HSV-1 infection does not augment EMT in CECs beyond putative partial transitions observed in $Ly6G^+$ CECs from healthy corneas. Accordingly, ectopic Ly6C expression observed in CECs following HSV-1 infection cannot be attributed to EMT alone.

VEGFA Enhances Epithelial Ly6C Expression in HSV-1 Keratitis

Although the proangiogenic effects of vascular endothelial growth factor A (VEGFA) are well established, VEGFA signaling is also linked to cellular reprogramming and transformation.[41] Moreover, VEGFA is directly induced by HSV-1 infection.[33] In order to assess the impact of HSV-1–associated VEGFA production on Ly6C expression in CECs, transgenic $Vegfa^{flox}$ mice expressing LoxP sequences flanking the *Vegfa* gene were utilized in parallel with the HSV-1 SC16 parental strain or a recombinant derivative expressing Cre recombinase under the infected cell protein 0 (*ICP0*) gene promoter as previously described.[34,36] In this model, $Vegfa^{flox}$ mice were ocularly infected with HSV-1 $ICP0^{WT}$ or the recombinant HSV-1 ICP0-Cre strain that ablates VEGFA in infected cells (Fig. 3A). This model reduces VEGFA protein levels in corneas of $Vegfa^{flox}$ mice by 75% to 80% at days 1 and 7 p.i. comparing the parental HSV-1 SC16 strain to the recombinant HSV-1 ICP0-Cre strain.[33,34]

Flow cytometry profiles of $EpCAM^+$ $CD45^-$ CECs derived from healthy corneas of $Vegfa^{flox}$ mice exhibited a negligible population of $Ly6G^+$ $Ly6C^+$ cells. However, a large reduction in the $Ly6G^+$ $Ly6C^+$ population was observed in CECs from $Vegfa^{flox}$ mice infected with HSV-1 ICP0-Cre relative to their respective counterparts infected with HSV-1 $ICP0^{WT}$ at day 6 p.i. (Fig. 3B). Higher numbers of CECs were recovered from female $Vefga^{flox}$ mice regardless of which virus was utilized, and a 50% decrease in the total number of CECs was observed in male mice infected with HSV-1 ICP0-Cre compared to HSV-1 $ICP0^{WT}$ (Fig. 3C). However, the sex-dependent number of total CECs recovered did not correlate with the overall Cre/VEGFA-dependent shift in the proportion of Ly6C expressing CECs following infection (Figs. 3D, 3E). Specifically, VEGFA ablation mediated by the HSV-1 ICP0-Cre virus diminished the proportion of Ly6G Ly6C coexpressing CECs by more than 50% compared to animals infected with the HSV-1 $ICP0^{WT}$ virus (Fig. 3E). Collectively, these data indicate that VEGFA signaling facilitates Ly6C upregulation in CECs following ocular HSV-1 infection.

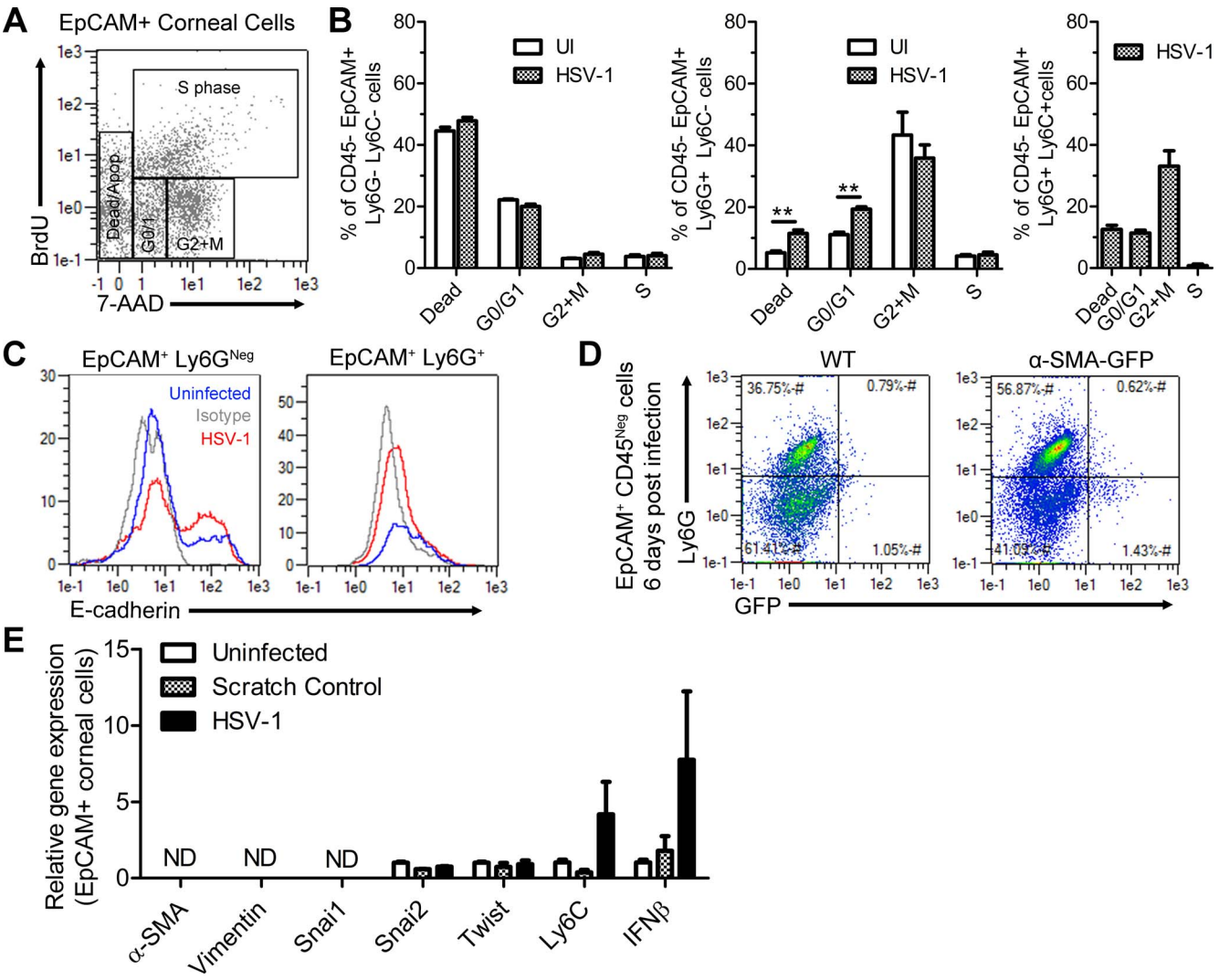

Figure 2. Ly6G$^+$ corneal epithelial cells exhibit a G2/M cell cycle bias and downregulate E-cadherin. EpCAM$^+$ cells isolated from healthy or HSV-1–infected corneas (day 6 p.i., 1×10^4 PFU HSV-1 McKrae per eye) were evaluated for evidence of epithelial–mesenchymal transition. (**A**) Cell cycle analysis showing representative plot of BrdU and 7-AA7 labeling. (**B**) Quantitative summary depicting the proportion of each EpCAM$^+$ CD45$^-$ corneal epithelial cell (CEC) subset in each phase of the cell cycle; subsets are based on presence or absence of Ly6C and Ly6G expression. Data reflect corneas from three male mice per group (six corneas) and two independent experiments analyzed using 2-way ANOVAs with Bonferroni posttests. (**C**) Flow cytometry histograms depicting E-cadherin expression in Ly6G$^+$ and Ly6G$^-$ CECs from healthy (*blue*) and HSV-1–infected (*red*) corneas. Isotype labeling (*gray*) was conducted using CECs from HSV-infected corneas. Data are representative of two independent experiments with three male mice per group. (**D**) Plot reflects CECs from HSV-infected WT and transgenic α-SMA-GFP reporter mice; data are representative of four or five male or female mice per group with two independent experiments. (**E**) Semiquantitative RT-PCR analysis of EMT-associated genes, *Ly6C1* and *IFNβ*. Data reflect reads of pooled EpCAM$^+$ cells from two male mice/sample ($n = 5$ pooled samples/group, two independent experiments). Expression is relative to *GAPDH* expression and normalized to uninfected controls using the $2^{-\Delta\Delta Ct}$ method.

Ly6C$^+$ Corneal Epithelial Cells Function as Antigen-Presenting Cells

To follow up on the unique myeloid-like phenotype observed in CECs following HSV-1 infection, we investigated their immunomodulatory potential. First, the impact of HSV-1 infection on the phagocytic capacity of CECs was assessed using pHrodo green–labeled *E. coli* bioparticles. The pH-dependent fluorescence shift observed upon bioparticle uptake was empirically determined using isolated neutrophils (Fig. 4A). Corneal digests were then incubated with bioparticles in vitro and compared to cell-only digests lacking bioparticles. Bioparticle uptake was evaluated in corneal digest subpopulations including EpCAM$^-$ CD45$^+$ leukocytes, EpCAM$^+$ CD45$^+$ Langerhans cells, and EpCAM$^+$ CD45$^-$ CECs (Fig. 4B). Bioparticles were endocytosed by each cell population as evidenced by the fluorescence shift upon bioparticle uptake (Fig. 4C). The phagocytic capacity of the Ly6C$^+$ CECs from HSV-1–infected corneas was uniform with the Ly6C$^-$ subset (Fig. 4C, right side). However, no quantitative differences were observed in the phagocytic capacity of cells from HSV-1–infected corneas relative to healthy control corneas based on the median fluorescence intensity (MFI) shift comparing cells with and without bioparticles (Fig. 4D).

Given the phagocytic nature of CECs, we subsequently evaluated major histocompatibility complex (MHC)-II expression and the immunomodulatory potential of these cells. A small population of CECs from healthy corneas expressed MHC-II, although HSV-1 infection led to a large upregulation of MHC-II specifically in the Ly6C$^+$ CEC population (Fig. 5A). Subsequent assessment of cosignaling molecules revealed that

Investigative Ophthalmology & Visual Science

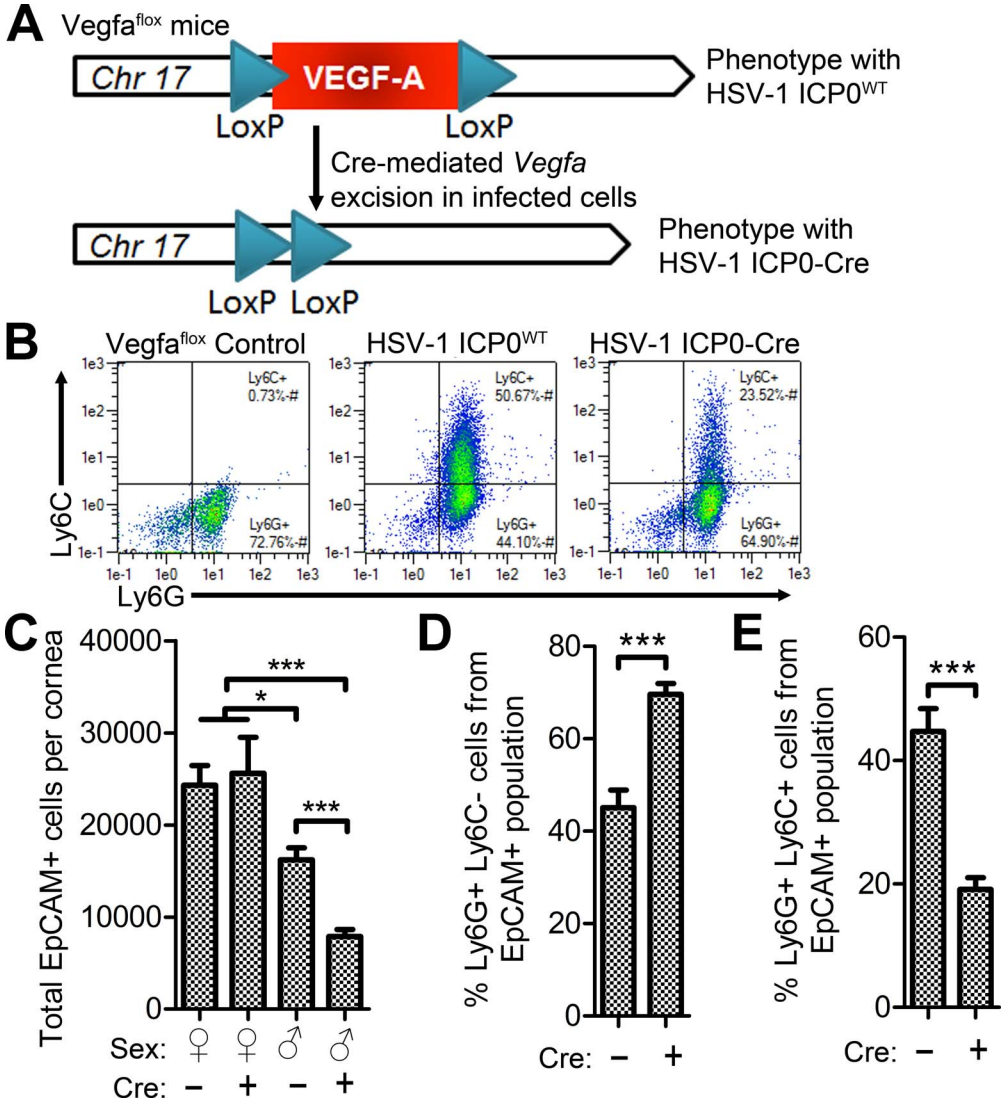

Figure 3. HSV-induced VEGFA signaling amplifies Ly6C expression in corneal epithelial cells. The impact of HSV-1–induced VEGFA production on Ly6C expression in CECs was assessed using transgenic VEGFA^{flox} mice ocularly infected bilaterally with 1×10^3 PFU HSV-1 SC16 or a recombinant derivative strain expressing Cre recombinase under the viral ICP0 promoter. (**A**) Cartoon depicts VEGFA ablation on chromosome 17 upon infection with the Cre-expressing virus (ICP0-Cre). (**B**) Representative plots of Ly6C and Ly6G expression in EpCAM$^+$ CD45$^-$ CECs derived from healthy or HSV-infected VEGFA^{flox} mice at day 6 p.i. (**C**) Quantitative summaries of the total number of EpCAM$^+$ CD45$^-$ CECs recovered from each cornea from male and female VEGFA^{flox} mice infected with ICP0^{WT} or ICP0-Cre virus (n = 8–10 corneas/group with three independent experiments). Sex-combined percentages of Ly6G$^+$ Ly6C$^-$ and Ly6G$^+$ Ly6C$^+$ CECs from mice in (**C**) are shown in (**D**, **E**), respectively. Data were analyzed by 2-way ANOVA in (**C**) or by Student's t-test in (**D**, **E**).

a subset of Ly6C$^+$ MHC-II$^+$ CECs from HSV-1–infected corneas express PD-L1 and low levels of CD86 (Fig. 5B).

Since a subpopulation of CECs express MHC-II, we next investigated the functional ability of CECs to prime CD4 T cells in vitro. Corneal digests from healthy or HSV-1–infected mice were separated by consecutive immunomagnetic isolation of CD45$^+$ and EpCAM$^+$ cells. Isolated leukocytes and CECs were then independently cocultured in vitro with FACS-purified transgenic OT-II CD4 T cells and $OVA_{323\text{-}339}$ peptide in the presence of acyclovir for 40 hours. EpCAM$^+$ CECs from HSV-1–infected corneas induced proliferation of OT-II CD4 T cells as evidenced by CFSE dilution (Figs. 5C, 5D). This effect was modest, however, compared to proliferation induced by CD45$^+$ cells from infected corneas (Figs. 5C, 5E). Further experiments were undertaken to characterize the phenotypic signature of the OT-II CD4 T cells following in vitro coculture. Analysis of proliferating OT-II CD4 T cells revealed no trends in CD25, CTLA-4, or TIM3 expression patterns (data not shown). However, a fraction of the proliferating OT-II CD4 T cells expressed IFNγ (Fig. 5F). In addition to inducing OT-II CD4 T cell proliferation, the corneal CD45$^+$ population uniquely induced FoxP3 expression in a subset of nonproliferating OT-II CD4 T cells (Fig. 5G). Taken together, our data provide evidence that CECs are amateur phagocytes capable of presenting antigen and modulating CD4 T cell responses.

Discussion

Ectopic Ly6G and Ly6C expression coincided with clear physiological changes impacting the molecular, cellular, and functional properties of isolated CECs. On the molecular level, the upregulation of chemokine receptors CCR2 and CX3CR1 as well as the loss of E-cadherin in Ly6G$^+$ CECs suggests that

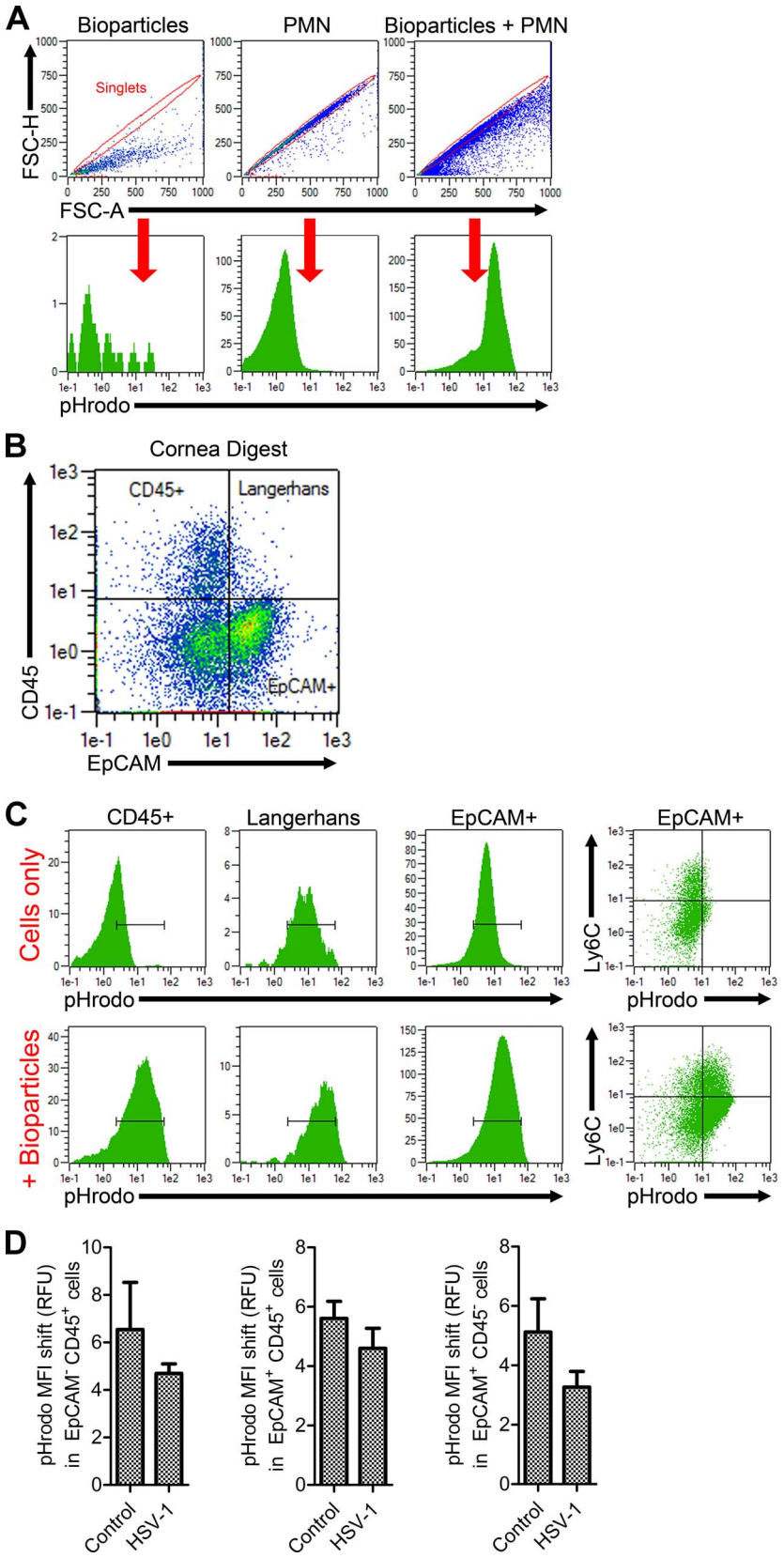

Figure 4. Corneal epithelial cells function as phagocytes. (**A**) Representative plots showing median fluorescence intensity (MFI) shift upon phagocytic uptake of pHrodo-green–labeled *E. coli* bioparticles in purified neutrophils (PMN). (**B**) Representative plots showing corneal digests segregated by CD45 and EpCAM labeling. (**C**) Representative histograms of cell populations from (**B**) isolated from HSV-1–infected cornea digests depicting median fluorescence intensity shift upon pHrodo-green bioparticle uptake (*bottom*) relative to no bioparticle (cell-only) populations (*top*). (**D**) Quantitative analysis of MFI shift from baseline (no bioparticles) upon uptake of pHrodo-green bioparticles in relative fluorescence units (RFU) for each cell population in (**B**) for healthy (control) and HSV-1–infected corneas. Shift reflects MFI change comparing corneal digests with and without bioparticles ($n = 7$–8 corneas from male or female mice per group with three independent experiments).

Investigative Ophthalmology & Visual Science

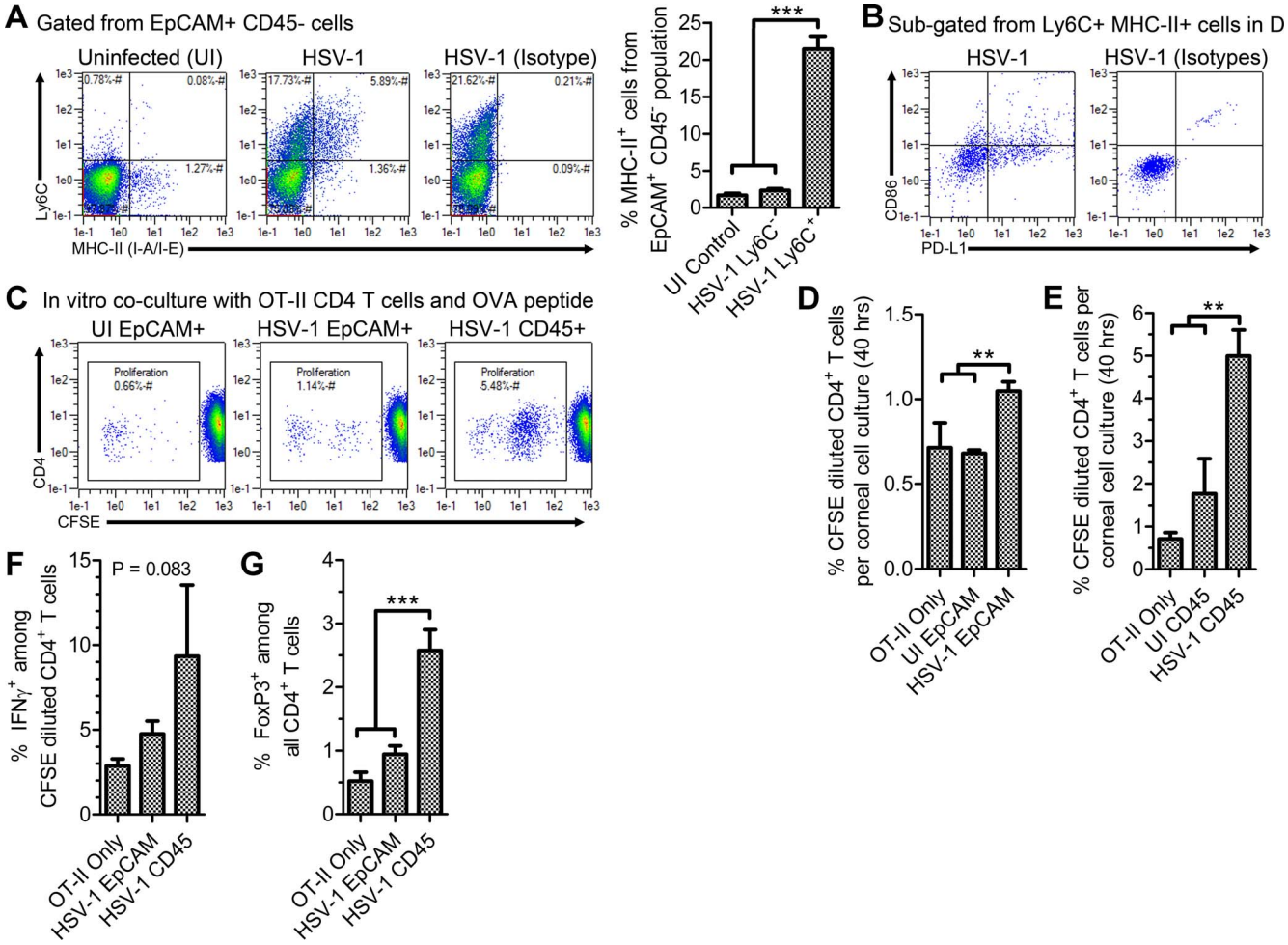

Figure 5. Corneal epithelial cells function as antigen-presenting cells during HSV-1 infection. EpCAM$^+$ CD45$^-$ CECs isolated from healthy or HSV-1–infected corneas were functionally evaluated for immunomodulatory effects. (**A**) Representative plots for analysis of MHC-II (I-A/I-E) expression in EpCAM$^+$ CD45$^-$ CECs from healthy control and HSV-1–infected corneas (n = 7–10 male or female corneas/group with three independent experiments). (**B**) Representative plots showing PD-L1 and CD86 expression (or isotype labeling) on Ly6C$^+$ MHC-II$^+$ CECs from HSV-1–infected corneas (data are representative of three male mice with two independent experiments). (**C**) Representative plots show proliferation of CFSE-labeled OT-II CD4 T cells cocultured with purified EpCAM$^+$ or CD45$^+$ cells from corneal digests in the presence of $OVA_{323-339}$ peptide. (**D**) Quantitative assessment of OT-II T cell proliferation induced by isolated EpCAM$^+$ cells (n = 6–8 cultures/group; two independent experiments utilizing cells from male and female corneas). (**E**) OT-II T cell proliferation induced by isolated CD45$^+$ cells (n = 2 uninfected, 4 HSV-1, and 6 OT-II-only cultures/group with two independent experiments utilizing cells from male and female corneas). (**F**) Percentage of proliferating (CFSE^{Low}) OT-II T cells expressing IFNγ following incubation with no exogenous cells, EpCAM$^+$ cells, or CD45$^+$ leukocytes from HSV-1–infected corneas. (**G**) Percentage of all OT-II T cells expressing FoxP3 following incubation with no cells, EpCAM$^+$ cells, or CD45+ leukocytes from HSV-1–infected corneas. For (**F**, **G**), n = 7 EpCAM$^+$ cultures, 4 CD45$^+$ cultures, and 6 OT-II-only cultures per group with two independent experiments utilizing cells from male and female corneas. Differences among groups in each part of the figure were calculated by 1-way ANOVA with Student-Newman-Keuls multiple comparison tests.

these cells may have enhanced motility. Indeed, CCR2 and CX3CR1 expression facilitate mucosal epithelial cell proliferation and mechanical wound closure in the airway and gut.[42–44] Furthermore, the EMT-inducing transcription factor Snai2 but not Snai1 was detectable by PCR in isolated EpCAM$^+$ cells from healthy and HSV-1–infected corneas. This finding is consistent with data showing nuclear accumulation of Snai2 but not Snai1 in CECs associated with corneal wound healing in vivo.[45] Progression of EMT in Ly6G$^+$ CECs is incomplete, as evidenced by lack of the mesenchymal markers α-SMA and vimentin. However, the observed phenotypic changes are consistent with a putative partial EMT event.

At the cellular level, Ly6G$^+$ CECs shift from the G0/G1 state observed in viable Ly6G$^-$ CECs to a G2/M-biased phenotype similar to what has been described during EMT-associated kidney fibrosis.[40] Importantly, the conspicuous absence of CD45, CD11b, CD11c, and CSF1R confirms that Ly6G$^+$ CECs are not of hematopoietic origin. Furthermore, it is well established that extracellular matrix remodeling impacts cellular physiology.[46] While the phenotypes observed in our study are likely exacerbated by corneal digestion, pathologic inflammatory conditions in vivo are intimately associated with loss of cell–cell contacts in the cornea through the actions of infiltrating leukocytes and matrix metalloproteinases.[47–51] Moreover, loss of cell–cell contacts in the corneal epithelium in vivo may enhance susceptibility to HSV-1 infection by liberating viral entry receptors normally sequestered within intercellular junctions.[52]

Many sexually dimorphic traits have been recognized in the cornea. As reviewed by Sullivan and colleagues,[53] these include differences in some corneal disease prevalence patterns as well as unique male/female gene expression

profiles involving a wide range of cellular dynamics in human CECs.[53,54] While we identified higher total numbers of CECs in female Vegfa^{flox} mice in the present investigation, it is important to note that Ly6C upregulation and immunomodulatory potential following HSV-1 infection were sex-independent. Our data are consistent with the sex-independent expression pattern of the related Ly6-family protein Slurp1, which is expressed in the healthy corneal epithelium but repressed by inflammation—including HSV-1 infection.[55,56]

Although the EMT-associated characteristics observed in isolated CECs did not differ as a result of HSV-1 infection as hypothesized, there was a clear functional difference endowing CECs from HSV-1–infected corneas with immunomodulatory potential. Corneal HSV-1 infection uniquely induced ectopic Ly6C upregulation in CECs through a VEGFA-linked mechanism. Consistent with this observation, the Ly6C$^+$ CEC population induced by HSV-1 infection coexpressed MHC-II. Previous studies have shown that CECs function as amateur phagocytes.[57,58] While CECs from both healthy and HSV-1–infected corneas were able to phagocytize particulate antigen, only CECs from HSV-1–infected corneas induced CD4 T cell proliferation above background levels.

Mucosal epithelial cells are increasingly recognized as enigmatic modulators of immune responses under pathologic conditions. This effect is mediated in part by aberrant MHC-II expression that is thought to promote peripheral tolerance.[59,60] Leukocytes can also transfer loaded peptide–MHC-II complexes to other cells via exosomes.[61,62] However, MHC-II expression on mucosal epithelial cells is not likely from exogenous sources, as evidence corroborates the ability of mucosal epithelial cells and other nonhematopoietic cells to independently process and present antigen through MHC-II.[60] Briefly, mucosal epithelial cells express the MHC-II transcriptional coactivator (CIITA) and various MHC-II alleles following IFNγ stimulation in vitro.[60,63] In addition, mucosal epithelial cells can also secrete immunomodulatory exosomes containing peptide–MHC-II complexes following IFNγ stimulation.[64] While MHC-II expression has been documented in the corneal epithelium following HSV-1 infection,[65–68] our study is the first to directly show a functional immunologic consequence of MHC-II expression in CECs using an HSV-independent model antigen system. Specifically, we show that MHC-II$^+$ CECs exhibit functional antigen-presenting capacities to naive CD4 T cells using an in vitro OT-II/OVA$_{323-339}$ peptide model. A similar study has shown that CD4 T cell priming by airway epithelial cells promotes a FoxP3$^+$ regulatory T cell phenotype.[69] Results from the current investigation show that CECs have limited ability to induce FoxP3 expression in naive OT-II CD4 T cells. However, interactions between naive CD4 T cells and MHC-II$^+$ CECs are unlikely to occur in vivo. Nonetheless, coexpression of MHC-II and PD-L1/CD86 on CECs, as observed in this study, may protect the cornea in situ by tolerizing infiltrating effector CD4 T cells. The functional implication of MHC-II expression by CECs necessitates further study to discern its impact on ocular surface disease.

The identification of CECs masquerading with multiple "myeloid" antigens warrants careful evaluation of experimental systems in which ectopic antigens may arbitrate inadvertent consequences. For example, neutralizing receptor/ligand interactions between PD-L1 and PD-1 during acute ocular HSV-1 infection exacerbates the severity of CD4 T cell–mediated corneal pathology.[70] Given that many MHC-II$^+$ CECs derived from HSV-1–infected corneas express PD-L1, it is tempting to speculate that MHC-II expression in the ocular mucosa serves as an additional mechanism of ocular immune privilege to limit CD4 T cell–driven immunopathology. Mucosal epithelial cells likely partner with their counterparts in the thymus to mediate peripheral and central tolerance, respectively. Moreover, ectopic Ly6G expression may be a surrogate marker for EMT in the mouse despite its universal recognition as a "myeloid" marker. We anticipate that our observation that VEGFA signaling coincides with Ly6C expression and enhanced immunomodulatory properties in CECs will be of considerable interest to those investigating epithelial malignancies, immune-evasion/-suppression, and tissue transplantation.

Although we have previously shown that HSV-1 drives VEGFA-dependent corneal lymphangiogenesis through the viral protein ICP4,[33] recent informatics approaches have validated single nucleotide polymorphisms in the *ICP4* gene as virulence determinants for HSV-1–associated corneal neovascularization.[71] From the standpoint of viral immune-evasion, the connections between HSV-1–associated VEGFA production and MHC-II expression in the corneal epithelium is significant and may serve to dampen local CD4 T cell responses during primary infection. Future studies are needed to elucidate this aspect of HSV-1 pathogenesis.

In summary, this study systematically characterizes a novel immunomodulatory CEC phenotype that may have implications for immune privilege, chronic inflammation, and tissue fibrosis. While HSV-1 infection does not elicit EMT in CECs above putative baseline levels detected in healthy corneal digests, it evokes immunomodulation through a VEGFA-linked mechanism. Moreover, the identification of CECs masquerading with multiple "myeloid" antigens warrants careful evaluation of flow cytometry data involving corneal digests.

Acknowledgments

The authors thank Stacey Efstathiou for providing the original stock of HSV-1 SC16-Cre.

Preliminary results from this study were presented at the annual meeting of the Association for Research in Vision and Ophthalmology, Baltimore, Maryland, United States, May 2017.

Supported by National Institutes of Health Grants R01 EY021238, T32 EY023202, and P30 EY021725. Additional support was provided by an unrestricted grant from Research to Prevent Blindness. The content of this manuscript is solely the responsibility of the authors and does not necessarily represent the official views of the National Institutes of Health or the National Eye Institute.

Disclosure: **D.J. Royer**, None; **M.H. Elliott**, None; **Y.Z. Le**, None; **D.J.J. Carr**, None

References

1. Hingorani M, Calder VL, Buckley RJ, Lightman SL. The role of conjunctival epithelial cells in chronic ocular allergic disease. *Exp Eye Res*. 1998;67:491–500.
2. Menon BB, Kaiser-Marko C, Spurr-Michaud S, Tisdale AS, Gipson IK. Suppression of Toll-like receptor-mediated innate immune responses at the ocular surface by the membrane-associated mucins MUC1 and MUC16. *Mucosal Immunol*. 2015;8:1000–1008.
3. Weitnauer M, Mijošek V, Dalpke AH. Control of local immunity by airway epithelial cells. *Mucosal Immunol*. 2016;9:287–298.
4. Loffredo LF, Abdala-Valencia H, Anekalla KR, Cuervo-Pardo L, Gottardi CJ, Berdnikovs S. Beyond epithelial-to-mesenchymal transition: common suppression of differentiation programs underlies epithelial barrier dysfunction in mild, moderate, and severe asthma. *Allergy*. 2017;72:1988–2004.
5. Turner JR. Intestinal mucosal barrier function in health and disease. *Nat Rev Immunol*. 2009;9:799–809.

6. De Paiva CS, Chotikavanich S, Pangelinan SB, et al. IL-17 disrupts corneal barrier following desiccating stress. *Mucosal Immunol*. 2009;2:243–253.
7. Wright NA, Pike C, Elia G. Induction of a novel epidermal growth factor-secreting cell lineage by mucosal ulceration in human gastrointestinal stem cells. *Nature*. 1990;343:82–85.
8. Blazejewska EA, Schlötzer-Schrehardt U, Zenkel M, et al. Corneal limbal microenvironment can induce transdifferentiation of hair follicle stem cells into corneal epithelial-like cells. *Stem Cells*. 2009;27:642–652.
9. Bonfanti P, Claudinot S, Amici AW, Farley A, Blackburn CC, Barrandon Y. Microenvironmental reprogramming of thymic epithelial cells to skin multipotent stem cells. *Nature*. 2010; 466:978–982.
10. Cursiefen C, Chen L, Saint-Geniez M, et al. Nonvascular VEGF receptor 3 expression by corneal epithelium maintains avascularity and vision. *Proc Natl Acad Sci U S A*. 2006;103: 11405–11410.
11. Pflugfelder SC, de Paiva CS, Li D-Q, Stern ME. Epithelial-immune cell interaction in dry eye. *Cornea*. 2008;27(suppl 1):S9–S11.
12. Niederkorn JY. Cornea: window to ocular immunology. *Curr Immunol Rev*. 2011;7:328–335.
13. Mashaghi A, Hong J, Chauhan SK, Dana R. Ageing and ocular surface immunity. *Br J Ophthalmol*. 2017;101:1–5.
14. Ksander BR, Kolovou PE, Wilson BJ, et al. ABCB5 is a limbal stem cell gene required for corneal development and repair. *Nature*. 2014;511:353–357.
15. Tiwari A, Loughner CL, Swamynathan S, Swamynathan SK. KLF4 plays an essential role in corneal epithelial homeostasis by promoting epithelial cell fate and suppressing epithelial–mesenchymal transition. *Invest Ophthalmol Vis Sci*. 2017;58: 2785–2795.
16. Ouyang H, Xue Y, Lin Y, et al. WNT7A and PAX6 define corneal epithelium homeostasis and pathogenesis. *Nature*. 2014;511:358–361.
17. Benítez-Del-Castillo J, Labetoulle M, Baudouin C, et al. Visual acuity and quality of life in dry eye disease: proceedings of the OCEAN group meeting. *Ocul Surf*. 2017;15:169–178.
18. Nieto MA, Huang RY-J, Jackson RA, Thiery JP. EMT: 2016. *Cell*. 2016;166:21–45.
19. Gilles C, Polette M, Piette J, Birembaut P, Foidart JM. Epithelial-to-mesenchymal transition in HPV-33-transfected cervical keratinocytes is associated with increased invasiveness and expression of gelatinase A. *Int J Cancer*. 1994;59: 661–666.
20. Horikawa T, Yang J, Kondo S, et al. Twist and epithelial-mesenchymal transition are induced by the EBV oncoprotein latent membrane protein 1 and are associated with metastatic nasopharyngeal carcinoma. *Cancer Res*. 2007;67:1970–1978.
21. Yang SZ, Zhang LD, Zhang Y, et al. HBx protein induces EMT through c-Src activation in SMMC-7721 hepatoma cell line. *Biochem Biophys Res Commun*. 2009;382:555–560.
22. Battaglia S, Benzoubir N, Nobilet S, et al. Liver cancer-derived hepatitis C virus core proteins shift TGF-beta responses from tumor suppression to epithelial-mesenchymal transition. *PLoS One*. 2009;4:e4355.
23. Kalluri R, Weinberg RA. The basics of epithelial-mesenchymal transition. *J Clin Invest*. 2009;119:1420–1428.
24. Schramm HM. Should EMT of cancer cells be understood as epithelial-myeloid transition? *J Cancer*. 2014;5:125–132.
25. Luddy KA, Robertson-Tessi M, Tafreshi NK, Soliman H, Morse DL. The role of toll-like receptors in colorectal cancer progression: evidence for epithelial to leucocytic transition. *Front Immunol*. 2014;5:429.
26. Johansson J, Tabor V, Wikell A, Jalkanen S, Fuxe J. TGF-β1-induced epithelial-mesenchymal transition promotes monocyte/macrophage properties in breast cancer cells. *Front Oncol*. 2015;5:3.
27. Pang M-F, Georgoudaki A-M, Lambut L, et al. TGF-β1-induced EMT promotes targeted migration of breast cancer cells through the lymphatic system by the activation of CCR7/CCL21-mediated chemotaxis. *Oncogene*. 2016;35:748–760.
28. Loughner CL, Bruford EA, McAndrews MS, Delp EE, Swamynathan S, Swamynathan SK. Organization, evolution and functions of the human and mouse Ly6/uPAR family genes. *Hum Genomics*. 2016;10:10.
29. Wang J-X, Bair AM, King SL, et al. Ly6G ligation blocks recruitment of neutrophils via a 2-integrin-dependent mechanism. *Blood*. 2012;120:1489–1498.
30. Jaakkola I, Merinen M, Jalkanen S, Hanninen A. Ly6C induces clustering of LFA-1 (CD11a/CD18) and is involved in subtype-specific adhesion of CD8 T cells. *J Immunol*. 2003;170:1283–1290.
31. Royer DJ, Carr MM, Gurung HR, Halford WP, Carr DJJ. The neonatal Fc receptor and complement fixation facilitate prophylactic vaccine-mediated humoral protection against viral infection in the ocular mucosa. *J Immunol*. 2017;199: 1898–1911.
32. Yokota T, Kawakami Y, Nagai Y, et al. Bone marrow lacks a transplantable progenitor for smooth muscle type α-actin-expressing cells. *Stem Cells*. 2006;24:13–22.
33. Wuest T, Zheng M, Efstathiou S, Halford WP, Carr DJJ. The herpes simplex virus-1 transactivator infected cell protein-4 drives VEGF-A dependent neovascularization. *PLoS Pathog*. 2011;7:e1002278.
34. Gurung HR, Carr MM, Carr DJJ. Cornea lymphatics drive the CD8+ T-cell response to herpes simplex virus-1. *Immunol Cell Biol*. 2017;95:87–98.
35. Li D-Q, Zhang L, Pflugfelder SC, et al. Short ragweed pollen triggers allergic inflammation through Toll-like receptor 4–dependent thymic stromal lymphopoietin/OX40 ligand/OX40 signaling pathways. *J Allergy Clin Immunol*. 2011;128:1318–1325.e2.
36. Proenca JT, Coleman HM, Connor V, Winton DJ, Efstathiou S. A historical analysis of herpes simplex virus promoter activation in vivo reveals distinct populations of latently infected neurones. *J Gen Virol*. 2008;89:2965–2974.
37. Swamydas M, Luo Y, Dorf ME, Lionakis MS. Isolation of mouse neutrophils. *Curr Protoc Immunol*. 2015;110:3.20.1–3.20.15.
38. Parkunan SM, Randall CB, Coburn PS, Astley RA, Staats RL, Callegan MC. Unexpected roles for toll-like receptor 4 and TRIF in intraocular infection with gram-positive bacteria. *Infect Immun*. 2015;83:3926–3936.
39. Merad M, Manz MG, Karsunky H, et al. Langerhans cells renew in the skin throughout life under steady-state conditions. *Nat Immunol*. 2002;3:1135–1141.
40. Lovisa S, LeBleu VS, Tampe B, et al. Epithelial-to-mesenchymal transition induces cell cycle arrest and parenchymal damage in renal fibrosis. *Nat Med*. 2015;21:998–1009.
41. Goel HL, Mercurio AM. VEGF targets the tumour cell. *Nat Rev Cancer*. 2013;13:871–882.
42. Lunndien MC, Mohammed KA, Nasreen N, et al. Induction of MCP-1 expression in airway epithelial cells: role of CCR2 receptor in airway epithelial injury. *J Clin Immunol*. 2002;22: 144–152.
43. Brand S, Sakaguchi T, Gu X, Colgan SP, Reinecker H. Fractalkine-mediated signals regulate cell-survival and immune-modulatory responses in intestinal epithelial cells. *Gastroenterology*. 2002;122:166–177.
44. Christensen PJ, Du M, Moore B, Morris S, Toews GB, Paine R. Expression and functional implications of CCR2 expression on murine alveolar epithelial cells. *Am J Physiol Lung Cell Mol Physiol*. 2004;286:L68–L72.

Investigative Ophthalmology & Visual Science

45. Aomatsu K, Arao T, Abe K, et al. Slug is upregulated during wound healing and regulates cellular phenotypes in corneal epithelial cells. *Invest Ophthalmol Vis Sci*. 2012;53:751–756.
46. Bonnans C, Chou J, Werb Z. Remodelling the extracellular matrix in development and disease. *Nat Rev Mol Cell Biol*. 2014;15:786–801.
47. Wagoner MD, Kenyon KR, Gipson IK, Hanninen LA, Seng WL. Polymorphonuclear neutrophils delay corneal epithelial wound healing in vitro. *Invest Ophthalmol Vis Sci*. 1984;25:1217–1220.
48. Riley GP, Harrall RL, Watson PG, Cawston TE, Hazleman BL. Collagenase (MMP-1) and TIMP-1 in destructive corneal disease associated with rheumatoid arthritis. *Eye*. 1995;9:703–718.
49. Smith VA, Rishmawi H, Hussein H, Easty DL. Tear film MMP accumulation and corneal disease. *Br J Ophthalmol*. 2001;85:147–153.
50. Mulholland B, Tuft SJ, Khaw PT. Matrix metalloproteinase distribution during early corneal wound healing. *Eye (Lond)*. 2005;19:584–588.
51. Lin M, Jackson P, Tester AM, et al. Matrix metalloproteinase-8 facilitates neutrophil migration through the corneal stromal matrix by collagen degradation and production of the chemotactic peptide Pro-Gly-Pro. *Am J Pathol*. 2008;173:144–153.
52. Chen C-H, Chen W-Y, Lin S-F, Wong RJ. Epithelial-mesenchymal transition enhances response to oncolytic herpesviral therapy through nectin-1. *Hum Gene Ther*. 2014;25:539–551.
53. Sullivan DA, Rocha EM, Aragona P, et al. TFOS DEWS II Sex, Gender, and Hormones Report. *Ocul Surf*. 2017;15:284–333.
54. Suzuki T, Richards SM, Liu S, Jensen RV, Sullivan DA. Influence of sex on gene expression in human corneal epithelial cells. *Mol Vis*. 2009;15:2554–2569.
55. Swamynathan S, Buela K-A, Kinchington P, et al. Klf4 regulates the expression of Slurp1, which functions as an immunomodulatory peptide in the mouse cornea. *Invest Ophthalmol Vis Sci*. 2012;53:8433–8436.
56. Swamynathan S, Delp EE, Harvey SAK, Loughner CL, Raju L, Swamynathan SK. Corneal expression of SLURP-1 by age, sex, genetic strain, and ocular surface health. *Invest Ophthalmol Vis Sci*. 2015;56:7888–7896.
57. Niederkorn JY, Peeler JS, Mellon J. Phagocytosis of particulate antigens by corneal epithelial cells stimulates interleukin-1 secretion and migration of Langerhans cells into the central cornea. *Reg Immunol*. 1989;2:83–90.
58. Stepp MA, Tadvalkar G, Hakh R, Pal-Ghosh S. Corneal epithelial cells function as surrogate Schwann cells for their sensory nerves. *Glia*. 2017;65:851–863.
59. Londei M, Lamb JR, Bottazzo GF, Feldmann M. Epithelial cells expressing aberrant MHC class II determinants can present antigen to cloned human T cells. *Nature*. 1984;312:639–641.
60. Kambayashi T, Laufer TM. Atypical MHC class II-expressing antigen-presenting cells: can anything replace a dendritic cell? *Nat Rev Immunol*. 2014;14:719–730.
61. Dolan BP, Gibbs KD, Ostrand-Rosenberg S. Tumor-specific CD4+ T cells are activated by "cross-dressed" dendritic cells presenting peptide-MHC class II complexes acquired from cell-based cancer vaccines. *J Immunol*. 2006;176:1447–1455.
62. Dubrot J, Duraes FV, Potin L, et al. Lymph node stromal cells acquire peptide–MHCII complexes from dendritic cells and induce antigen-specific CD4+ T cell tolerance. *J Exp Med*. 2014;211:1153–1166.
63. Mulder DJ, Pooni A, Mak N, Hurlbut DJ, Basta S, Justinich CJ. Antigen presentation and MHC class II expression by human esophageal epithelial cells: role in eosinophilic esophagitis. *Am J Pathol*. 2011;178:744–753.
64. Van Niel G, Mallegol J, Bevilacqua C, et al. Intestinal epithelial exosomes carry MHC class II/peptides able to inform the immune system in mice. *Gut*. 2003;52:1690–1697.
65. el-Asrar AM, van den Oord JJ, Billiau A, Desmet V, Emarah Mh, Missotten L. Recombinant interferon-gamma induces HLA-DR expression on human corneal epithelial and endothelial cells in vitro: a preliminary report. *Br J Ophthalmol*. 1989;73:587–590.
66. Fahy GT, Hooper DC, Easty DL. Antigen presentation of herpes simplex virus by corneal epithelium–an in vitro and in vivo study. *Br J Ophthalmol*. 1993;77:440–444.
67. Twardy BS, Channappanavar R, Suvas S. Substance P in the corneal stroma regulates the severity of herpetic stromal keratitis lesions. *Invest Ophthalmol Vis Sci*. 2011;52:8604–8613.
68. Buela K-AG, Hendricks RL. Cornea-infiltrating and lymph node dendritic cells contribute to CD4+ T cell expansion after herpes simplex virus-1 ocular infection. *J Immunol*. 2015;194:379–387.
69. Gereke M, Jung S, Buer J, Bruder D. Alveolar type II epithelial cells present antigen to CD4+ T cells and induce Foxp3^{+} regulatory T cells. *Am J Respir Crit Care Med*. 2009;179:344–355.
70. Jun H, Seo SK, Jeong H-Y, et al. B7-H1 (CD274) inhibits the development of herpetic stromal keratitis (HSK). *FEBS Lett*. 2005;579:6259–6264.
71. Lee K, Kolb AW, Larsen I, Craven M, Brandt CR. Mapping murine corneal neovascularization and weight loss virulence determinants in the herpes simplex virus 1 genome and the detection of an epistatic interaction between the UL and IRS/US regions. *J Virol*. 2016;90:8115–8131.

Investigative Ophthalmology & Visual Science